Apoptosis (2015) 20:1187–1199
DOI 10.1007/s10495-015-1152-y

ORIGINAL PAPER

Berberine prevents nitric oxide-induced rat chondrocyte apoptosis and cartilage degeneration in a rat osteoarthritis model via AMPK and p38 MAPK signaling

Yan Zhou[1] · Shi-Qing Liu[1] · Ling Yu[1] · Bin He[1] · Shi-Hao Wu[2] · Qi Zhao[1] · Shao-Qiang Xia[1] · Hong-Jun Mei[3]

Published online: 17 July 2015

Abstract Chondrocyte apoptosis is an important mechanism involved in osteoarthritis (OA). Berberine (BBR), a plant alkaloid derived from Chinese medicine, is characterized by multiple pharmacological effects, such as anti-inflammatory and anti-apoptotic activities. This study aimed to evaluate the chondroprotective effect and underlying mechanisms of BBR on sodium nitroprusside (SNP)-stimulated chondrocyte apoptosis and surgically-induced rat OA model. The in vitro results revealed that BBR suppressed SNP-stimulated chondrocyte apoptosis as well as cytoskeletal remodeling, down-regulated expressions of inducible nitric oxide synthase (iNOS) and caspase-3, and up-regulated Bcl-2/Bax ratio and Type II collagen (Col II) at protein levels, which were accompanied by increased adenosine monophosphate-activated protein kinase (AMPK) phosphorylation and decreased phosphorylation of p38 mitogen-activated protein kinase (MAPK). Furthermore, the anti-apoptotic effect of BBR was blocked by AMPK inhibitor Compound C (CC) and adenosine-9-β-D-arabino-furanoside (Ara A), and enhanced by p38 MAPK inhibitor SB203580. In vivo experiment suggested that BBR ameliorated cartilage degeneration and exhibited an anti-apoptotic effect on articular cartilage in a rat OA model, as demonstrated by histological analyses, TUNEL assay and immunohistochemical analyses of caspase-3, Bcl-2 and Bax expressions. These findings suggest that BBR suppresses SNP-stimulated chondrocyte apoptosis and ameliorates cartilage degeneration via activating AMPK signaling and suppressing p38 MAPK activity.

Keywords Berberine · Osteoarthritis · Chondrocyte · Sodium nitroprusside · Apoptosis

✉ Shi-Qing Liu
liusqrm@163.com

[1] Department of Orthopedics, Central Laboratory, Renmin Hospital, Wuhan University, Wuhan 430060, People's Republic of China

[2] Department of Psychiatry, Renmin Hospital, Wuhan University, Wuhan 430060, People's Republic of China

[3] Department of Orthopedics, Wuhan NO. 5 Hospital, Wuhan 430050, People's Republic of China

Introduction

Osteoarthritis (OA) is characterized by the degeneration of articular cartilage and subchondral bone and accompanied by joint pain, swelling and stiffness, leading to joint dysfunction [1, 2]. Many different factors, including genetics, lifestyle and joint instability contribute to the onset and progression of OA, which greatly affects quality of life in elder population [3]. The pathological process of OA involves in articular cartilage chondrocyte apoptosis, chondrocyte phenotype loss and overproduction of pro-inflammatory mediators, such as tumor necrosis factor-α, interleukin (IL)-1β, nitric oxide (NO), and prostaglandins [4–7]. Specifically, NO donor sodium nitroprusside (SNP) is commonly known as an inducing and modulating agent to trigger chondrocyte apoptosis [8, 9]. The relationship between chondrocyte apoptosis and the severity and progression of OA has been confirmed [10–12]. Thus, at early stage of OA, inhibiting chondrocyte apoptosis may be a potential strategy against the progression of cartilage degeneration.

Adenosine monophosphate-activated protein kinase (AMPK) is an enzyme comprised of α, β and γ subunits [13]. Previous studies have shown that activation of AMPK is involved in a variety of pathological conditions such as

ischemia, glucose deprivation, oxidative stress, starvation, and adiponectin-induced degradation of cartilage matrix [14, 15]. It has also been demonstrated that activation of AMPK protects against hydrogen peroxide-induced osteoblast apoptosis probably through autophagy induction and nicotinamide adenine dinucleotide phosphate maintenance [16]. Mitogen-activated protein (MAP) kinases consist of p38 MAPK, extracellular signal-regulated kinase p44/42 MAPK, and c-Jun N-terminal kinase [17]. It has been proved that activation of p38 MAPK has participated in chondrocyte apoptosis [18]. On the other hand, inhibition of p38 MAPK has been shown to exhibit protective effect on cartilage degradation in different animal models [19].

Berberine chloride (BBR, structure shown in Fig. 1) is a botanical alkaloid derived from several species of medicinal herbs, including *Coptis chinensis* and *Berberis aristate* [20]; BBR has shown multiple pharmacological effects, including antibiotic [21], anti-inflammatory [22], anticancer [23], anti-oxidative [24], and anti-apoptotic [25] effects. Recent studies have demonstrated that BBR decreases IL-1β-stimulated glycosaminoglycan release and NO production, and down-regulates matrix metalloproteinases expression in vitro and in vivo [26, 27]. BBR was also shown to protect articular cartilage from degeneration via activating Akt/p70S6K/S6 signaling pathway in IL-1β-induced articular chondrocytes and in a rat OA model [28]. Nevertheless, few data is available on the therapeutic mechanism for BBR on SNP-stimulated chondrocyte apoptosis. The purpose of this study is to determine whether BBR inhibits SNP-stimulated rat chondrocyte apoptosis and ameliorates cartilage degeneration in a rat OA model, and to elucidate the underlying mechanism associated with AMPK and p38 MAPK signaling pathways.

Materials and methods

Reagents

BBR (purity ≥98 %) and AMPK inhibitor Compound C (CC) were obtained from Sigma-Aldrich (St. Louis, MO, USA). The stock solution of BBR was prepared by dissolving in methanol to a final concentration of 0.2 % methanol in the medium, and the medium with 0.2 % methanol was used as the control. The p38 MAPK inhibitor SB203580, AMPK inhibitor adenosine-9-β-D-arabino-furanoside (Ara A), and rabbit antibodies against caspase-3, Bax and Bcl-2 were obtained from Calbiochem (San Diego, CA, USA). Cell counting kit-8 (CCK-8) was obtained from Dojindo Laboratories (Kumamoto, Japan). Annexin V-fluorescein isothiocyanate (FITC)/propidium iodide (PI) apoptosis kit was supplied by MultiSciences Biotech Co.,Ltd (Hangzhou, China). Dulbecco's modified Eagle's medium (DMEM)/F12 and trypsin were purchased from Hyclone (USA). Type II collagenase was from Invitrogen (California, USA). Fetal bovine serum (FBS) and penicillin/streptomycin were obtained from Gibco-BRL (Maryland, USA). Type II collagen (Col II), inducible nitric oxide synthase (iNOS), glyceraldehyde-3-phosphate dehydrogenase (GAPDH), phospho-AMPK (p-AMPK), AMPK, p-p38 MAPK, and p38 MAPK antibodies were obtained from Abcam (Cambridge, UK). SNP was purchased from Youcare Pharmaceutical Group Co., Ltd (Beijing, China). All of the other chemicals and reagents were of analytical grade.

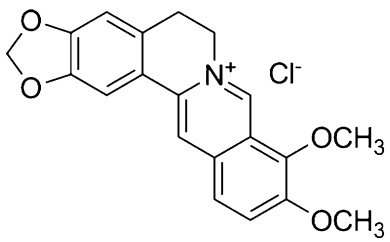

Fig. 1 The structure of berberine chloride (BBR)

Cell isolation and culture

Primary articular chondrocytes were isolated from the knee joints of newborn (5 days old) Sprague-Dawley (SD) rats (from the Center for Animal Experiment/ABSL-III Laboratory of Wuhan University, Wuhan, China). Rat articular cartilage was separated under sterile conditions and rinsed in phosphate-buffered saline (PBS) three times. The cartilage was sectioned into pieces measuring about 0.5–1 mm^3. The cartilage tissue was digested with 0.25 % Trypsin & 0.02 % EDTA for 60 min, and then placed in petri dishes containing 0.2 % type II collagenase at 37 °C incubator for 4–5 h until most of the cartilage was visible floc. The cell suspension was collected by gently pipetting and centrifuged at 1000 rpm for 5 min to collect the cell pellet. Then cells were resuspended in DMEM/F12 complete culture medium (containing 10 % FBS and 100 units/ml of penicillin and streptomycin). The cells were cultured at 37 °C in a humidified 5 % CO_2 incubator. The primary cells were observed under an inverted microscope and passaged upon reaching 80 % confluence. The second generation chondrocytes were identified by toluidine blue staining. All of the protocols were approved by the Institutional Ethics Committee of Medical School, Wuhan University.

Cell stimulation and treatment

The third passage chondrocytes were resuspended in DMEM/F12 supplemented with 10 % FBS, 100 unit/ml

penicillin and 100 unit/ml streptomycin for 24 h when cells were adherent at 70–80 % confluency. Then, chondrocytes were stimulated with different concentrations of BBR in the presence and absence of CC (1 μM), Ara A (0.5 mM) or SB203580 (10 μM) respectively for 2 h before 0.75 mM SNP co-treatment for 24 h.

Evaluation of cell viability by CCK-8 assay

The third passage chondrocytes were cultured in 96-well plates (0.5×10^4/well) for 24 h, and then exposed to different concentrations of BBR (0, 25, 50, 75, 100, 150, and 200 μM) for 12, 24 and 48 h. The medium was removed and 100 μl of 10 % CCK-8 solution was added to each well for 1–4 h incubation at 37 °C. Then the optical density value was determined by ELISA reader (Bio-Tek, Model EXL800, USA) at 450 nm.

Evaluation of apoptosis

According to the manufacturer's instructions, flow cytometry analysis with Annexin V-FITC/PI kit was carried out to explore chondrocyte apoptosis rates. Briefly, chondrocytes and cultural supernatants were collected by centrifugation at 1000 rpm for 5 min, washed with cold PBS two times, and gently resuspended in 500 μl binding buffer. Then 5 μl PI solution and 5 μl Annexin V-FITC were added and incubated with cells in the dark for 15 min. Apoptosis rates were analyzed on a FACScan flow cytometer (Becton-Dickinson, USA).

Immunofluorescence assay

The vimentin cytoskeleton was detected by immunofluorescence assays. Adherent chondrocytes at 70 % confluency were cultured on glass coverslips in 6-well plates and starved for 12 h before treatment. Chondrocytes were washed with 37 °C PBS twice, fixed with 4 % paraformaldehyde for 20 min, permeabilized with 0.5 % Triton X-100 buffer (Beyotime, Jiangsu, China) at room temperature for 5 min, and blocked with 1 % bovine serum albumin at 4 °C for 10 min. The cells were washed with PBS three times after each step. Then, chondrocytes were incubated with rabbit anti-vimentin antibody (Santa Cruz Biotech, Dallas, USA; 1:100 dilution) at room temperature for 2 h. After washing with PBS, chondrocytes were incubated with Fluorescein Isothiocyanate-labeled secondary antibody (Boster Biological Engineering, Wuhan, China; 1:100 dilution) in the dark for 1 h. Nuclei were counter-stained with DAPI (KeyGEN Biotech, Nanjing, China) for 10 min, and images were visualized by an Olympus microscope (Olympus Corporation, Tokyo, Japan).

Western blot analysis

Proteins in cultured chondrocytes were isolated using a total protein extraction kit according to the manufacturer's instructions. The extracted cellular proteins were loaded on a sodium dodecyl sulfate-polyacrylamide gel electrophoresis. After electrophoresis, proteins were transferred to polyvinylidene difluoride membranes previously soaked with methanol for 5 min. After briefly washing in Tris-buffered saline with Tween-20 (TBST), the membranes were blocked with 5 % (w/v) nonfat dry milk in TBST at room temperature for 1 h. Then the membranes were incubated with primary antibodies against caspase-3, Bcl-2, Bax, Col II, iNOS, p-AMPK, AMPK, p-p38 MAPK, p38 MAPK, and GAPDH overnight at 4 °C. Following washing with TBST, the membranes were incubated with the respective peroxidase-conjugated secondary antibodies for 1 h. Chemiluminescent signals were visualized with enhanced chemiluminescence Western blot detection reagent (Amersham Biosciences, Piscataway, NJ, USA). Immunoblot bands were analyzed using Odyssey infrared imaging system (LI-COR, NE, USA). Data were expressed as the relative differences between control and treated cells after normalization to GAPDH expression.

Establishment of a rat OA model

Twenty male SD rats (200–250 g body weight) obtained from the Center for Animal Experiment/ABSL-III Laboratory of Wuhan University were used for this study. The animals were accommodated to standard laboratory conditions (12 h light and dark cycle at 20–24 °C, and humidity 50–55 %) for 1 week and allowed free access to food and water, and then allocated randomly into four groups ($n = 5$) including sham-operated, OA-induction, OA + BBR (Low-dose), and OA + BBR (High-dose) groups. The animals were anaesthetized intraperitoneally with trichloroacetaldehyde hydrate (300 mg/kg) in sterile saline. The OA model was established in the right knee joint by anterior cruciate ligament transection combined with medial menisci resection (ACLT + MMx) as previously described [29]. After surgery, the joint was irrigated with sterile saline solution, and both capsule and skin were closed with 4-0 nylon sutures. For the sham-operated group, the wounds were sutured after exposing the knee joint cartilage surface. The animals were injected intramuscularly with antibiotics (1.0–1.3 mg/cefotiam hydrochloride) for 3 days after surgery. From the first week after surgery, the rats were placed in an electric rotating cage. The cage was 20 cm in diameter and 22 cm in transverse diameter, with constantly rotating activity (speed 15 rpm) for half an hour per day. The running distance of each rat was roughly 280 m per day according

to the equation: S (m) = π × d × n × 30, where d and n represent the diameter and the speed, respectively. From the 4th week after surgery, low- and high-dose BBR treatment groups received an injection of 50 μl of 100 and 200 μM BBR. Meanwhile, the sham-operated and OA-induction groups received an injection of 50 μl PBS into the right knee joint. The animals were sacrificed by cardiac exsanguinations at the 10th week after surgery. All animal studies were conducted with approval from the Animal Care and Use Committee of Medical School, Wuhan University.

Histological analysis

The right knee joints were immediately fixed in 4 % paraformaldehyde after dissection for 24 h, decalcified in Calci-Clear slow solution [10 % (w/v) EDTA, pH 7.4] for at least 3 weeks and then embedded in paraffin wax. Hematoxylin and Eosin (H&E) staining was performed on 5 μm serial sagittal sections of cartilaginous tissue. Semi-quantitative histopathological grading was performed by two blinded observers according to a modified Mankin scoring system [30]. Safranin-O-Fast green staining was performed to assess cartilage proteoglycan content [31].

TUNEL assay

TUNEL assays were performed using an in situ apoptosis detection kit according to the manufacturer's instructions (KeyGEN Biotech, Nanjing, China). The serial sagittal sections of cartilaginous tissue were digested with 20 μg/ml proteinase K (Dako, Glostrup, Denmark) for 15 min, immersed in 3 % hydrogen peroxide for 5 min and incubated with terminal deoxynucleotidyl transferase at 37 °C for 1 h. Then the sections were incubated with anti-digoxigenin-peroxidase antibody at 37 °C for 30 min, visualized by diaminobenzidine and counterstained with haematoxylin. Chondrocytes with brown nuclei were assessed as positive. The percentage of apoptotic chondrocytes was evaluated using three randomly selected high power fields (×200) in each slide from four groups.

Immunohistochemical analysis

Immunohistochemical analyses were performed on articular cartilage to investigate the protein expressions of caspase-3, Bcl-2, Bax, and Col II. An immunohistochemical SP assay was conducted according to the manufacturer's instructions. The serial sagittal sections of cartilaginous tissue were incubated with primary antibodies: caspase-3 (1:200 dilution), Bax (1:100), Bcl-2 (1:100), and Col II (1:200). The images of the sections were captured using an optical microscope with ×200 and ×400 magnification. The positive expression of caspase-3, Bcl-2, Bax, and Col II appeared brown. The integrated optical density (IOD) of immunostaining was calculated using Image-Pro Plus 6.0 image analysis software (Media Cybernetics Co., USA).

Statistical analysis

Data were presented as mean ± SEM. The differences between each group were compared for statistical significance using one-way ANOVA analysis and Student's *t* test with SPSS 13.0 statistical software. Statistical significance was defined as $P < 0.05$. All statistical tests were performed using GraphPad Prism software, version 5.0 (San Diego, CA, USA).

Results

Effects of BBR on chondrocyte viability

The viability effect of BBR on normal chondrocytes was evaluated by CCK-8 assay with increasing concentrations (25–200 μM) for 12, 24 and 48 h (Fig. 2). Cell viability was calculated as percentage of the control group. The results indicated that BBR showed no significant cytotoxicity against normal chondrocytes except for 200 μM at 48 h (**$P < 0.01$).

Effects of BBR on SNP-stimulated chondrocyte apoptosis

The percentages of chondrocytes in the four quadrants are representative of necrotic cells (Q1 Annexin V-FITC+/PI+), late apoptotic cells (Q2 Annexin V-FITC+/PI+), live cells (Q3 Annexin V-FITC−/PI−), and early apoptotic cells (Q4 Annexin V-FITC+/PI−). As shown in Fig. 3, the percentage of apoptotic chondrocytes treated with 0.75 mM SNP was 59.8 ± 6.7 %, which was significantly

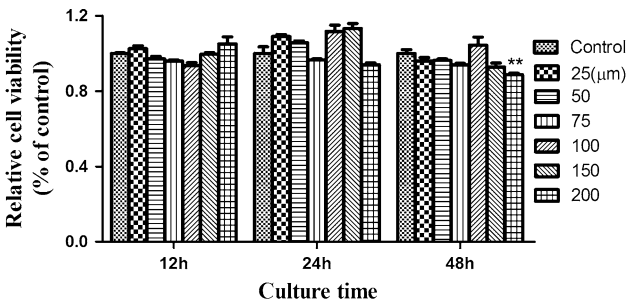

Fig. 2 CCK8 assay results. The rat chondrocytes were exposed to BBR at concentrations ranging from 25 to 200 μM for 12, 24 and 48 h. Each column represents mean ± SEM ($n = 6$). **$P < 0.01$ versus the control group

higher than that of the control group (***$P < 0.001$). After treated with increasing concentrations of BBR (25–75 μM), the proportion of apoptotic chondrocytes were decreased progressively. And the apoptotic cells were markedly decreased by 75 μM BBR compared with that of 100 μM BBR.

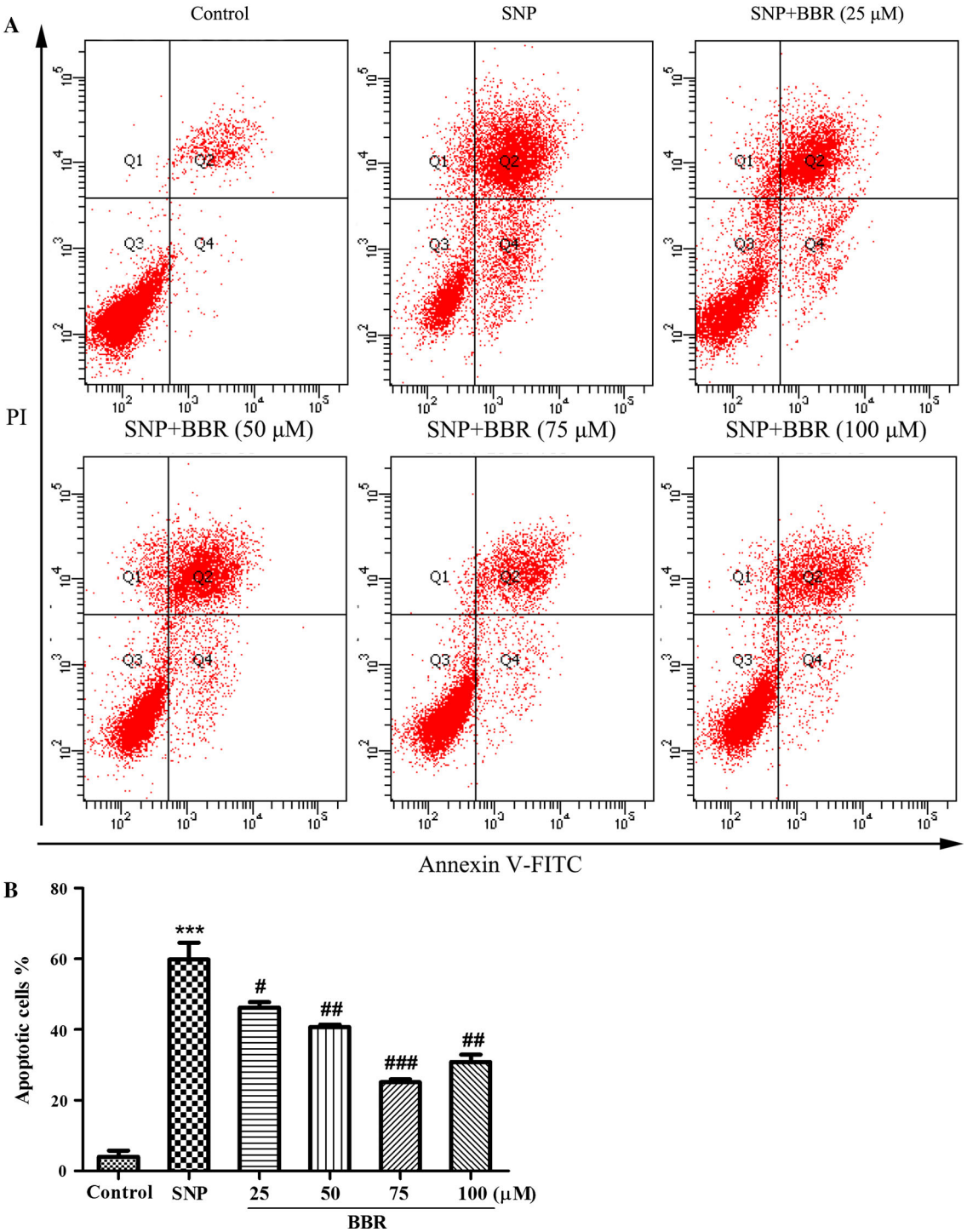

Fig. 3 Effects of BBR on SNP-stimulated chondrocyte apoptosis. **a** Flow cytometry with Annexin V-FITC/PI dual staining of chondrocytes pre-incubated with BBR at concentrations ranging from 25 to 100 μM for 2 h before 0.75 mM SNP co-treatment for 24 h. **b** Each *column* represents mean ± SEM ($n = 3$). ***$P < 0.001$ versus the control group; $^{\#}P < 0.05$, $^{\#\#}P < 0.01$ and $^{\#\#\#}P < 0.001$ versus the SNP group

Effects of BBR on SNP-stimulated cytoskeletal remodeling

Fluorescent microscopy was used to image the cytoskeleton of chondrocytes incubated with Vimentin-Trakcer Green (Fig. 4). In the control group, regular vimentin filaments as well as uniformly intermediate filament cytoskeleton were observed. SNP shortened vimentin filaments and induced cell shrinkage, which could be prevented by pretreatment with 75 μM BBR. However, compared with the BBR (75 μM) + SNP group, the percentages of remodeling chondrocytes were increased by the treatment of BBR plus AMPK inhibitor CC (1 μM) or Ara A (0.5 mM) ($^{\$\$}P < 0.01$ and $^{\$\$\$}P < 0.001$), and decreased by the treatment of BBR plus p38 MAPK inhibitor SB203580 (10 μM) ($^{\$\$}P < 0.01$).

BBR attenuated SNP-stimulated chondrocyte apoptosis through AMPK and p38 MAPK signaling pathways

To explore the mechanism of BBR decreasing chondrocyte apoptosis, the protein expressions of cleaved caspase-3, Bcl-2, Bax, and iNOS were determined. As shown in Fig. 5b, c, compared with the control group, the expressions of cleaved caspase-3 and iNOS increased and Bcl-2/Bax ratio decreased in SNP-stimulated chondrocytes. These trends were reversed by administration of BBR at concentrations ranging from 25 to 75 μM. However, compared with the BBR + SNP groups, pretreatment with BBR plus CC (1 μM) or Ara A (0.5 mM) decreased Bcl-2/Bax ratio and increased cleaved caspase-3 and iNOS expressions (Figs. 5b, c, 6a). On the other hand, pretreatment with BBR plus SB203580 (10 μM) increased Bcl-2/Bax ratio and decreased cleaved caspase-3 expression (Fig. 6a). The results indicated that BBR attenuated SNP-stimulated chondrocyte apoptosis probably through AMPK and p38 MAPK signaling.

BBR increased p-AMPK and decreased p-p38 MAPK in SNP-stimulated chondrocytes

The total and phosphorylation levels of AMPK and p38 MAPK in different groups were evaluated with Western blot. As illustrated in Figs. 5d and 6b, the expression of p-AMPK decreased in 0.75 mM SNP-stimulated chondrocytes, while pretreatment with BBR blocked the SNP-stimulated down-regulation of p-AMPK and BBR reversed the SNP-stimulated up-regulation of p-p38 MAPK. The AMPK inhibitor CC (1 μM) or Ara A (0.5 mM) attenuated the BBR-mediated increase in p-AMPK expression, and the p38 MAPK inhibitor SB203580 (10 μM) obviously decreased the p-p38 MAPK expression compared with the BBR-mediated regulation. The protein levels of total AMPK and p38 MAPK in different groups showed no obvious changes. As shown in Fig. 5a, the expression of Col II in SNP-stimulated rat chondrocytes appeared to be up-regulated by administration of 25 and 75 μM BBR in a dosage-dependent manner. The addition of CC (1 μM) attenuated the BBR-mediated increase in Col II expression.

Effects of BBR on histopathology in OA cartilage

Histopathological changes in each group were concentrated on the cartilage surface and matrix layer (Fig. 7a). In the sham-operated group, articular cartilage possessed regular morphological structure, while the surface of articular cartilage was irregular and the intensity of Safranin O staining was lower in the OA-induction group. With intra-articular injection of BBR (100 and 200 μM), the rat knee articular cartilage thickness had increased significantly, and the cartilage degradation was apparently ameliorated in a dosage-dependent manner. The statistical results on the modified Mankin scores in different groups are shown in Fig. 7b. The severity of the OA + BBR (100 and 200 μM) groups was much lower than that of the OA-induction group ($^{\#}P < 0.05$ and $^{\#\#}P < 0.01$).

Effects of BBR on chondrocyte apoptosis in vivo

As shown by TUNEL assay in Fig. 7a, few TUNEL-positive chondrocytes were found in the sham-operated group, whereas ubiquitously and strongly expressed in the OA-induction group. The number of TUNEL-positive chondrocytes was apparently reduced with intra-articular injection of BBR in a dosage-dependent manner. The statistical results of the percentage of TUNEL-positive chondrocytes (number of positive cells/number of total cells) in four groups are shown in Fig. 7b, and there was statistical significance between the OA + BBR (100 and 200 μM) groups and the OA-induction group ($^{\#}P < 0.05$ and $^{\#\#}P < 0.01$).

Effects of BBR on caspase-3, Bax, Bcl-2, and Col II proteins in a rat OA model

As shown in Fig. 8, positive expressions of caspase-3, Bax, Bcl-2, and Col II in representative cartilage sections appeared brown. Immunohistochemical analyses revealed that the IOD of caspase-3 and Bax expressions in the superficial layer of articular cartilage increased significantly in the OA-induction group ($^{***}P < 0.001$, versus the sham-operated group), and gradually decreased by intra-articular injection of BBR from 100 to 200 μM ($^{\#}P < 0.05$, $^{\#\#}P < 0.01$ and $^{\#\#\#}P < 0.001$, versus the OA-induction group). The expression of Bcl-2 was progressively enhanced in the OA + BBR (100 and 200 μM)

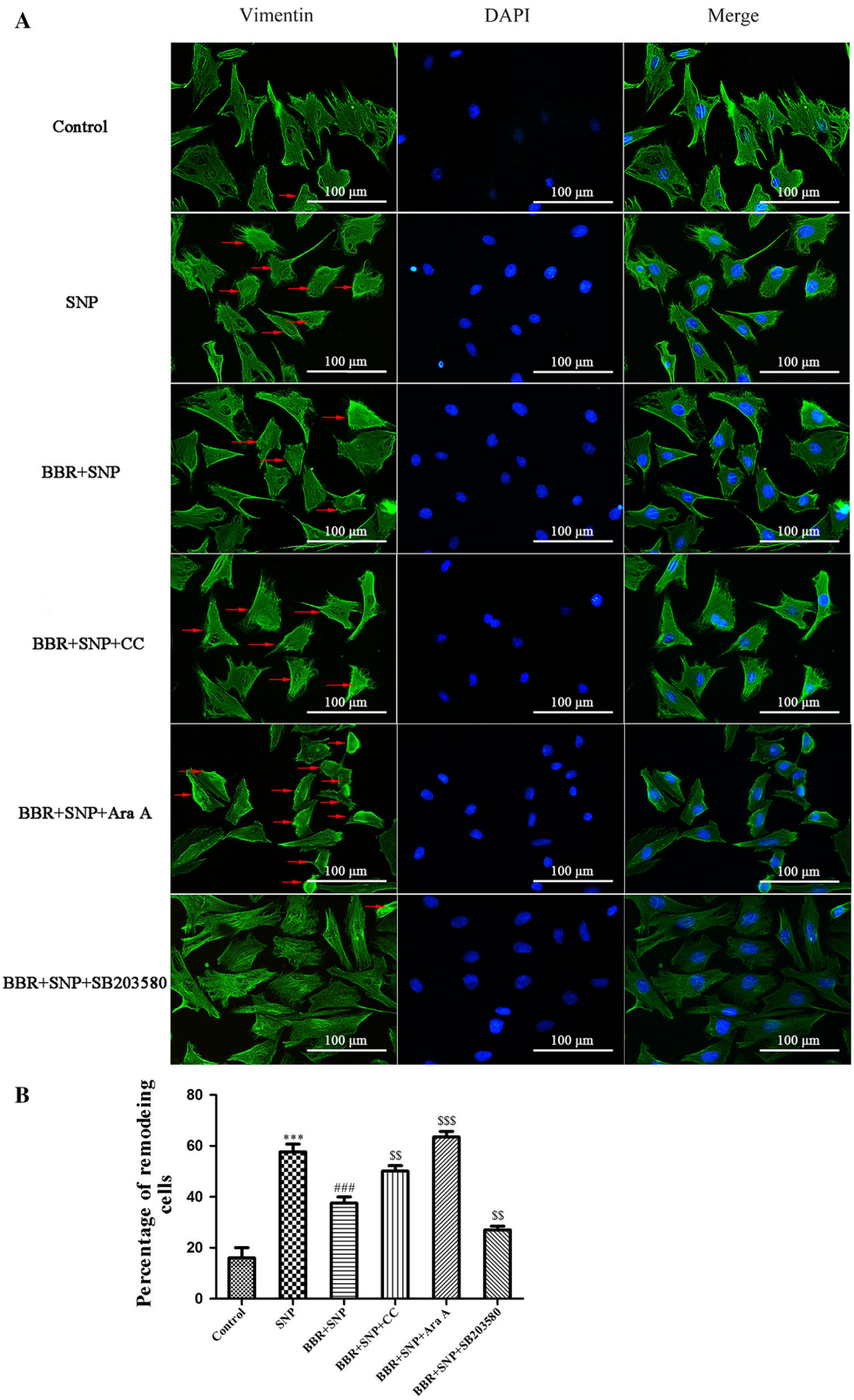

Fig. 4 Effects of BBR on cytoskeletal remodeling in SNP-stimulated chondrocytes. **a** Fluorescent images with Vimentin-Trakcer Green of chondrocytes pre-incubated with 75 μM BBR in the presence and absence of the AMPK inhibitor CC (1 μM), Ara A (0.5 mM) or the p38 MAPK inhibitor SB203580 (10 μM) for 2 h before 0.75 mM SNP co-treatment for 24 h. *Red arrows* represent chondrocytes with short vimentin filaments and shrinkage. **b** Each column represents mean ± SEM of the percentages of remodeling chondrocytes ($n = 3$). $^{***}P < 0.001$ versus the control group; $^{\#\#\#}P < 0.001$ versus the SNP group; $^{\$\$}P < 0.01$ and $^{\$\$\$}P < 0.001$ versus the SNP + BBR (75 μM) group (Color figure online)

groups compared with the OA-induction group ($^{\#\#}P < 0.01$ and $^{\#\#\#}P < 0.001$). Meanwhile, compared with the OA-induction group, the Col II protein expression in growth plate and articular cartilage in the OA + BBR (100 and 200 μM) groups was up-regulated in a dosage-dependent manner ($^{\#}P < 0.05$ and $^{\#\#}P < 0.01$).

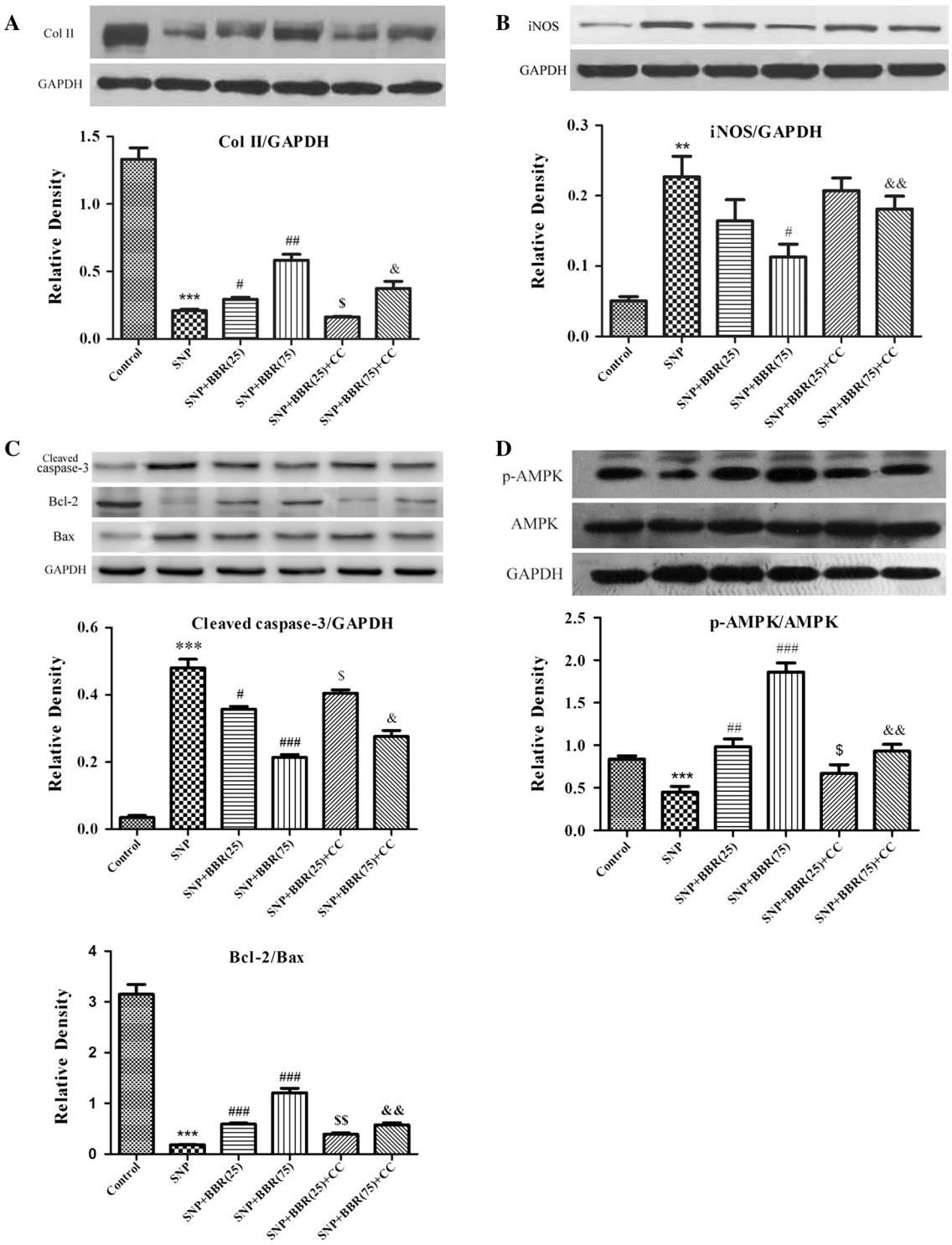

Fig. 5 AMPK signaling pathway is involved in the anti-apoptotic effect of BBR on SNP-stimulated rat chondrocytes. Chondrocytes were pre-incubated with BBR (25 and 75 μM) in the presence and absence of the AMPK inhibitor CC (1 μM) for 2 h before 0.75 mM SNP co-treatment for 24 h. **a** The protein level of Col II expression and ratio of Col II/GAPDH. **b** The protein level of iNOS expression and ratio of iNOS/GAPDH. **c** The protein expressions of cleaved caspase-3, Bcl-2 and Bax, and ratios of cleaved caspase-3/GAPDH and Bcl-2/Bax. **d** The protein expressions of p-AMPK and AMPK and ratio of p-AMPK/AMPK. Each column represents mean ± SEM ($n = 3$). $^{**}P < 0.01$ and $^{***}P < 0.001$ versus the control group; $^{\#}P < 0.05$, $^{\#\#}P < 0.01$ and $^{\#\#\#}P < 0.001$ versus the SNP group; $^{\$}P < 0.05$ and $^{\$\$}P < 0.01$ versus the SNP + BBR (25 μM) group; $^{\&}P < 0.05$ and $^{\&\&}P < 0.01$ versus the SNP + BBR (75 μM) group

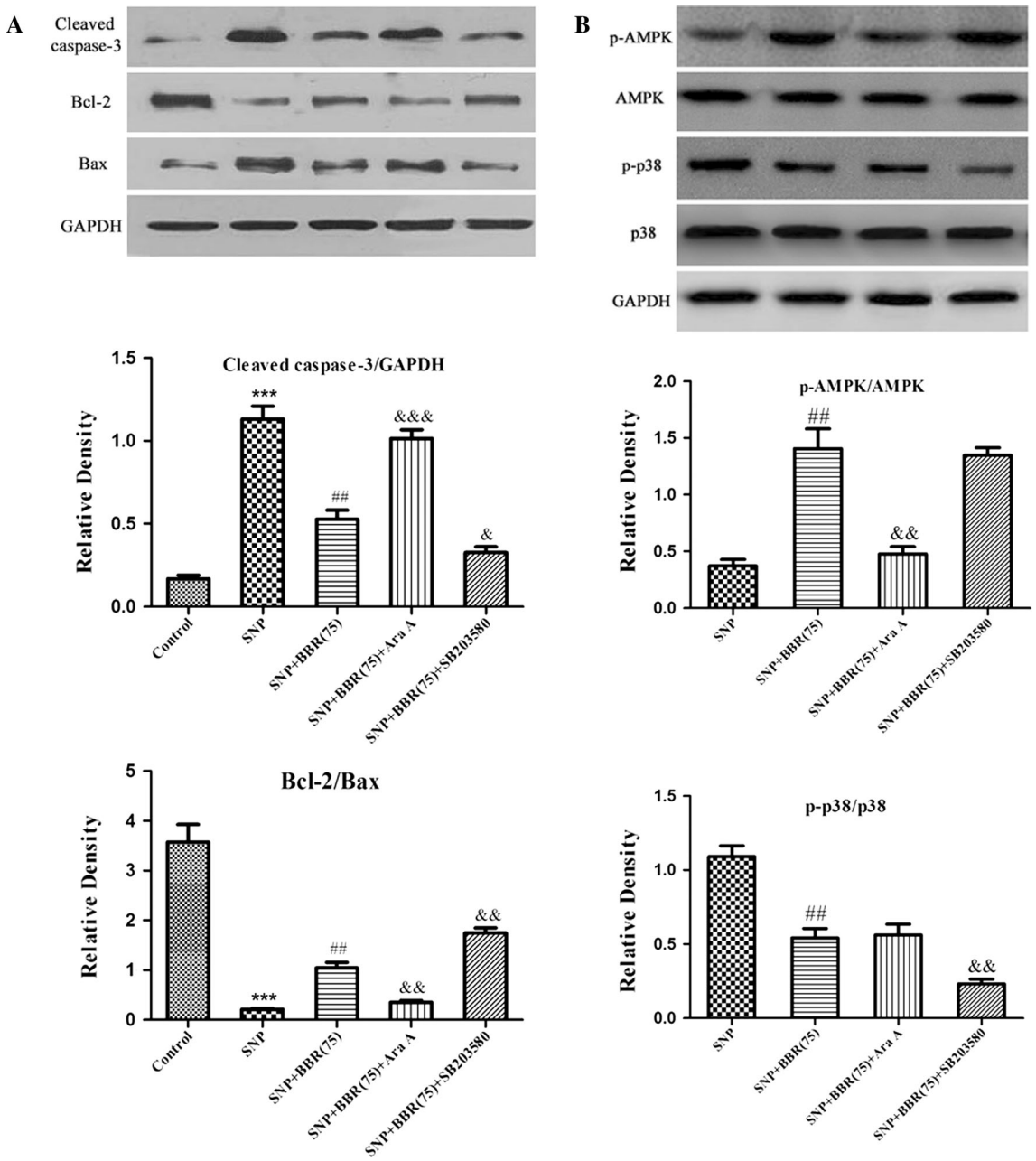

Fig. 6 BBR suppressed SNP-stimulated rat chondrocyte apoptosis through both AMPK and p38 MAPK signaling pathways. Chondrocytes were pre-incubated with BBR (75 μM) in the presence and absence of the AMPK inhibitor Ara A (0.5 mM) or the p38 MAPK inhibitor SB203580 (10 μM) for 2 h before 0.75 mM SNP co-treatment for 24 h. **a** The protein expressions of cleaved caspase-3, Bcl-2 and Bax and ratios of cleaved caspase-3/GAPDH and Bcl-2/Bax. **b** The protein expressions of p-AMPK, AMPK, p-p38 MAPK, and p38 MAPK and ratios of p-AMPK/AMPK and p-p38 MAPK/p38 MAPK. Each column represents mean ± SEM ($n = 3$). $^{***}P < 0.001$ versus the control group; $^{\#\#}P < 0.01$ versus the SNP group; $^{\&}P < 0.05$, $^{\&\&}P < 0.01$ and $^{\&\&\&}P < 0.001$ versus the SNP + BBR (75 μM) group

Discussion

In this study, we investigated the effects of BBR on SNP-stimulated rat chondrocyte apoptosis, as well as on articular cartilage in a surgically-induced rat OA model, and the underlying mechanism with AMPK and p38 MAPK signaling pathways. The results demonstrate that BBR attenuated SNP-stimulated chondrocyte apoptosis and elicited cartilage protective effect possibly through its anti-apoptotic effect via activating AMPK signaling and suppressing p38 MAPK activity.

BBR is an isoquinoline alkaloid, the anti-apoptotic property of which has been applied extensively to a variety of diseases [25, 32, 33]. Attenuating the process of apoptosis

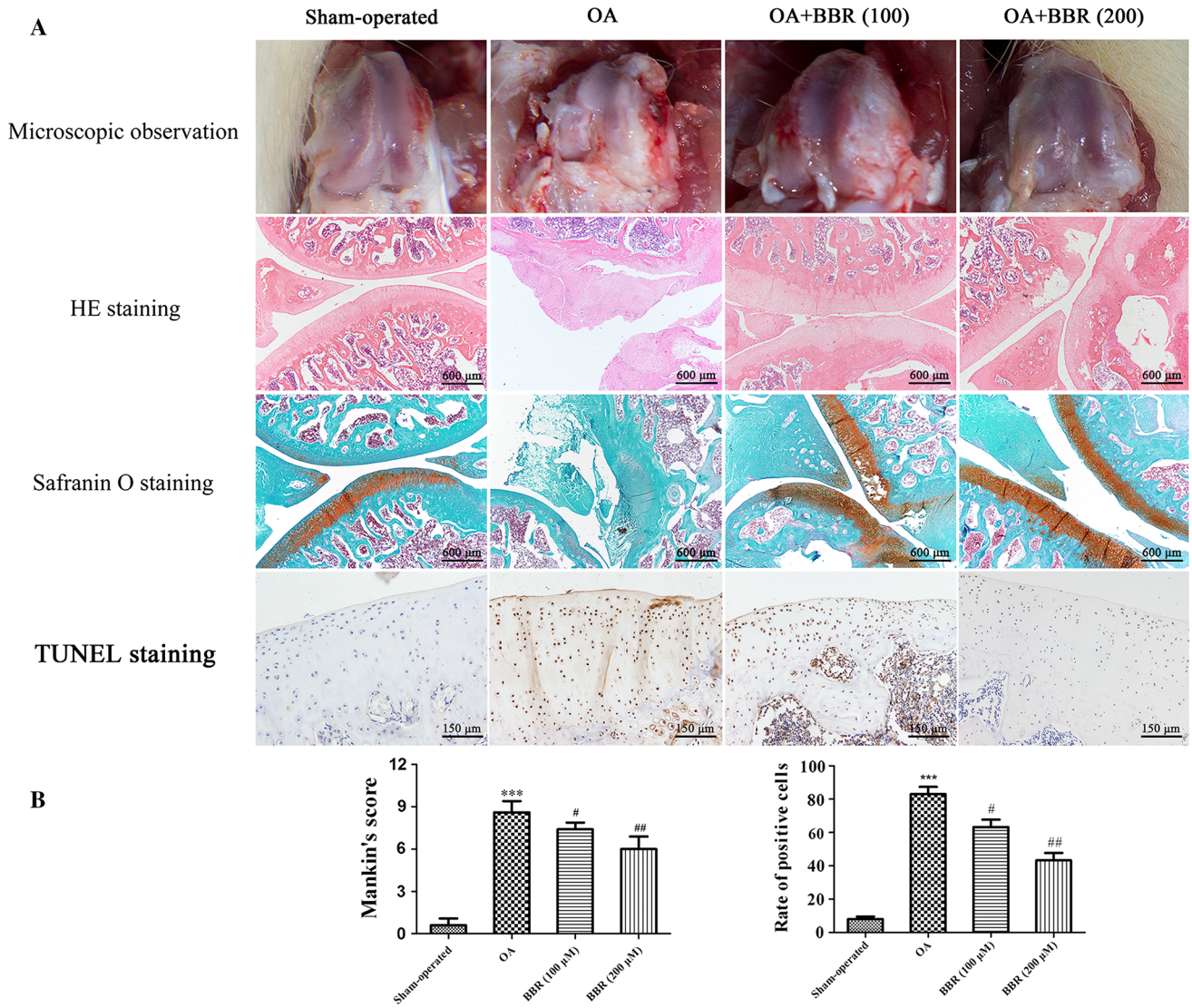

Fig. 7 **a** Gross morphology, histological analyses of rat articular cartilage by H&E and Safranin O staining (original magnification ×40) and representative TUNEL-stained sections (original magnification ×200) in each group. **b** Mankin's score and apoptotic index in four groups. Each *column* represents mean ± SEM in Mankin's score ($n = 5$) and in TUNEL-positive chondrocytes ($n = 3$). $^{***}P < 0.001$ versus the sham-operated group; $^{\#}P < 0.05$ and $^{\#\#}P < 0.01$ versus the OA-induction group

could ameliorate the progression of cartilage degeneration [8, 34]. SNP is a fast acting vasodilator that is often used to be an external NO donor for clinical and basic research [35, 36]. In this study, 0.75 mM fresh SNP was used to induce chondrocyte apoptosis and the apoptotic rate was about 59 %, and 75 μM BBR could significantly reduce SNP-induced chondrocyte apoptosis than 100 μM BBR. We think the result could be mainly ascribed to the following aspects. First, in this study, definite concentrations of BBR exhibited the anti-apoptotic and chondroprotective effects on OA chondrocytes similar to previous studies [27, 28]. Second, the interaction between BBR and SNP could be mutual influence and restriction so as to achieve dynamic balance for treatment. BBR and SNP may have common therapeutic targets on rat chondrocytes. And the relevant mechanisms deserve further study. Third, the co-treatment of a high concentration of BBR (100 μM) and 0.75 mM SNP could enlarge the toxic effect of BBR and reveal the rare effect of BBR on promoting apoptosis according to previous study [37]. In this study, the results of flow cytometry test and Western blot have demonstrated that BBR reversed SNP-induced chondrocyte apoptosis, and down-regulated the protein expressions of Bax and caspase-3, while up-regulated Bcl-2 expression in cultured chondrocytes. Elevated level of NO released upon SNP stimulation triggers iNOS expression in PC12 cells [38]. The iNOS expression is strongly up-regulated at a high level in OA chondrocytes and plays a vital role in OA progression [39]. In this study, we

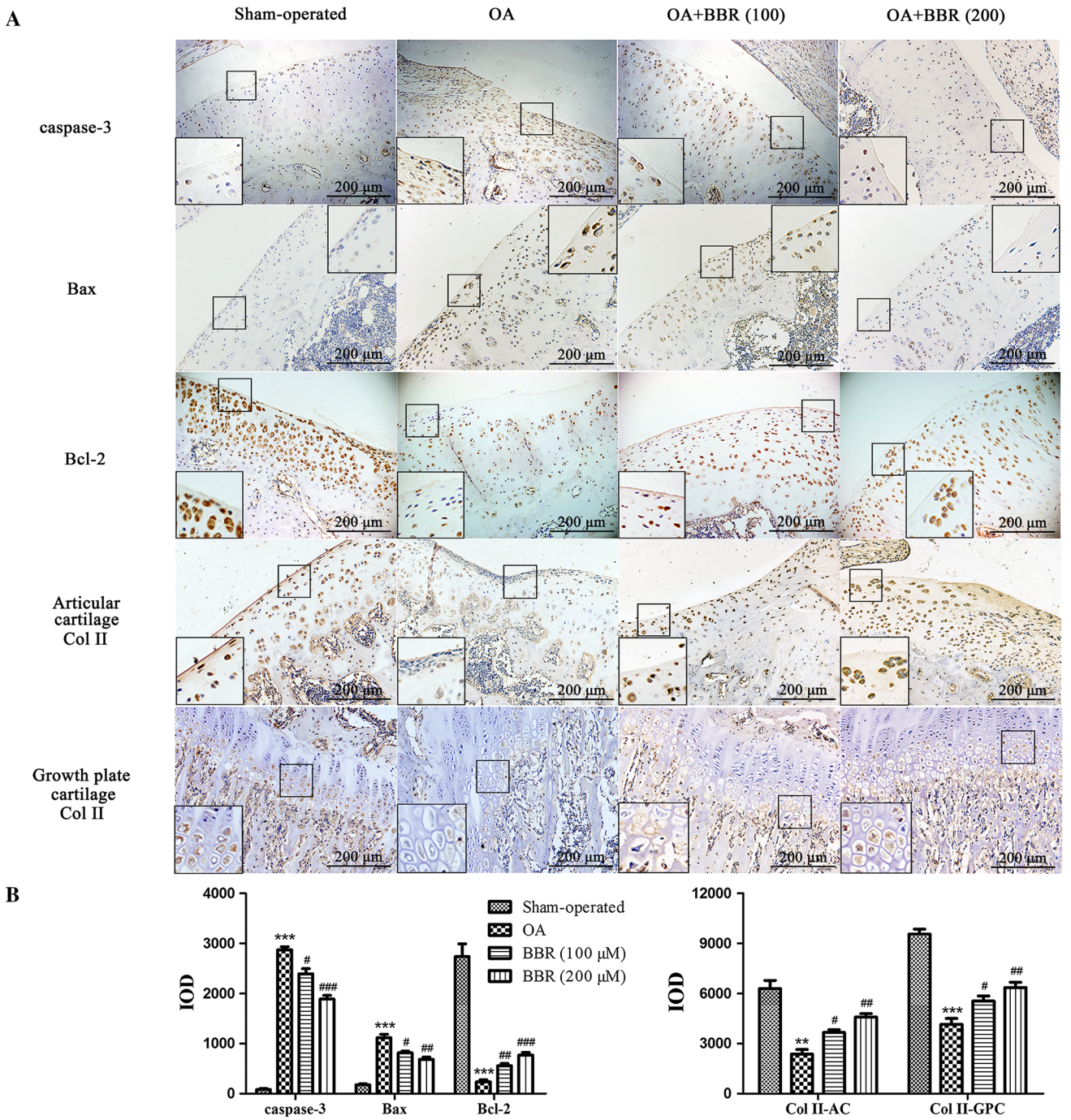

Fig. 8 **a** Immunohistochemical analyses of caspase-3, Bax, Bcl-2, and Col II expressions in each group (original magnification ×200 and zoom-in areas magnification ×400). **b** Each column represents mean ± SEM of IOD ($n = 3$). $^{**}P < 0.01$ and $^{***}P < 0.001$ versus the sham-operated group; $^{\#}P < 0.05$, $^{\#\#}P < 0.01$ and $^{\#\#\#}P < 0.001$ versus the OA-induction group

confirmed that BBR could suppress SNP-induced iNOS protein expression in chondrocytes. Chondrocyte homeostasis requires an intact cytoskeleton and extracellular matrix synthesis, and the disruption of vimentin network might contribute to cartilage degeneration [40]. We observed that BBR could reverse the SNP-induced cytoskeletal remodeling to some extent.

In the present study, it is worth mentioning that BBR attenuated SNP-stimulated chondrocyte apoptosis via activating AMPK signaling and suppressing p38 MAPK activity. Recent evidences suggested that activated AMPK was involved in the anti-apoptotic effect on potential chondroprotection [41, 42], and chondrocyte apoptosis was accompanied by increased phosphorylation of p38 MAPK

[17]. Earlier studies have demonstrated that BBR could block apoptosis in prevention of endothelial dysfunction associated with diabetes and cardiovascular disease in part through AMPK activation [43, 44]. BBR down-regulated p38 MAPK signaling pathway in colonic macrophages and epithelial cells in response to dextran sulfate sodium treatment in vivo [45]; BBR attenuated left ventricular remodeling and cardiomyocyte apoptosis associated with enhanced autophagy through inhibition of p38 MAPK signalling pathway [33]. Nevertheless, the precise mechanisms of AMPK and p38 MAPK regulate the chondroprotective effect of BBR are not fully understood.

The results in this study suggest that BBR markedly up-regulated Bcl-2/Bax ratio, down-regulated active caspase-3 protein expression, increased Col II protein expression, and enhanced AMPK phosphorylation, compared with the combined treatment of BBR and AMPK inhibitor CC or Ara A. Pretreatment with BBR plus p38 MAPK inhibitor SB203580 effectively blocked the phosphorylation of p38 MAPK compared with the BBR-mediated regulation. In addition, compared with BBR treatment, the SNP-induced cytoskeletal remodeling was effectively reversed by the treatment of BBR plus SB203580, and the treatment of BBR plus CC or Ara A could disrupt the vimentin network. Taken together, the results indicate that the chondroprotective effect of BBR may be attributed to the AMPK- and p38 MAPK-mediated anti-apoptotic effect in SNP-stimulated rat chondrocytes.

Our data also suggested that BBR attenuated articular chondrocyte apoptosis and ameliorated cartilage degeneration in a rat ACLT + MMx OA model. The in vivo study showed that the Mankin scores were significantly lower and the higher matrix production and thicker cartilage layer were observed in the BBR-injected groups compared with the OA-induction group; BBR exhibited an anti-apoptotic effect on articular cartilage in a rat OA model as evidenced by TUNEL assay. In addition, immunohistochemical analyses showed that intra-articular injection of BBR decreased Bax and caspase-3 protein expressions, increased Bcl-2 expression, and enhanced Col II synthesis in both growth plate and articular cartilage. Thus, BBR has a potential therapeutic ability for cartilage degeneration in a rat OA model.

In summary, the present study suggests for the first time that BBR suppressed NO-induced chondrocyte apoptosis in vitro and exerted chondroprotective effect in vivo via activating AMPK signaling and suppressing p38 MAPK activity. These findings suggest the potential therapeutic value of BBR in the treatment of OA. Additional in vivo studies are required further to validate these mechanisms.

Acknowledgments We gratefully acknowledge Erping Yang for his excellent technical assistance.

Compliance with ethical standards

Conflict of interest All authors declared no potential conflicts of interest.

References

1. Aicher WK, Rolauffs B (2014) The spatial organisation of joint surface chondrocytes: review of its potential roles in tissue functioning, disease and early, preclinical diagnosis of osteoarthritis. Ann Rheum Dis 73:645–653
2. Thysen S, Luyten FP, Lories RJ (2015) Targets, models and challenges in osteoarthritis research. Dis Model Mech 8:17–30
3. Johnson VL, Hunter DJ (2014) The epidemiology of osteoarthritis. Best Pract Res Clin Rheumatol 28:5–15
4. Terkeltaub R, Yang B, Lotz M, Liu-Bryan R (2011) Chondrocyte AMP-activated protein kinase activity suppresses matrix degradation responses to proinflammatory cytokines interleukin-1beta and tumor necrosis factor alpha. Arthritis Rheum 63:1928–1937
5. Wang X, Hunter D, Xu J, Ding C (2015) Metabolic triggered inflammation in osteoarthritis. Osteoarthritis Cartilage 23:22–30
6. Liu-Bryan R, Terkeltaub R (2015) Emerging regulators of the inflammatory process in osteoarthritis. Nat Rev Rheumatol 11:35–44
7. Lee AS, Ellman MB, Yan D, Kroin JS, Cole BJ et al (2013) A current review of molecular mechanisms regarding osteoarthritis and pain. Gene 527:440–447
8. Liang Q, Wang XP, Chen TS (2014) Resveratrol protects rabbit articular chondrocyte against sodium nitroprusside-induced apoptosis via scavenging ROS. Apoptosis 19:1354–1363
9. Ryu JS, Jung YH, Cho MY, Yeo JE, Choi YJ et al (2014) Co-culture with human synovium-derived mesenchymal stem cells inhibits inflammatory activity and increases cell proliferation of sodium nitroprusside-stimulated chondrocytes. Biochem Biophys Res Commun 447:715–720
10. Uehara Y, Hirose J, Yamabe S, Okamoto N, Okada T et al (2014) Endoplasmic reticulum stress-induced apoptosis contributes to articular cartilage degeneration via C/EBP homologous protein. Osteoarthritis Cartilage 22:1007–1017
11. Hui W, Young DA, Rowan AD, Xu X, Cawston TE, et al (2014) Oxidative changes and signalling pathways are pivotal in initiating age-related changes in articular cartilage. Ann Rheum Dis. doi:10.1136/annrheumdis-2014-206295
12. Battistelli M, Salucci S, Olivotto E, Facchini A, Minguzzi M et al (2014) Cell death in human articular chondrocyte: a morpho-functional study in micromass model. Apoptosis 19:1471–1483
13. Mihaylova MM, Shaw RJ (2011) The AMPK signalling pathway coordinates cell growth, autophagy and metabolism. Nat Cell Biol 13:1016–1023
14. Dasgupta B, Milbrandt J (2007) Resveratrol stimulates AMP kinase activity in neurons. Proc Natl Acad Sci USA 104:7217–7222
15. Kang EH, Lee YJ, Kim TK, Chang CB, Chung JH et al (2010) Adiponectin is a potential catabolic mediator in osteoarthritis cartilage. Arthritis Res Ther 12:R231
16. She C, Zhu LQ, Zhen YF, Wang XD, Dong QR (2014) Activation of AMPK protects against hydrogen peroxide-induced osteoblast apoptosis through autophagy induction and NADPH maintenance: new implications for osteonecrosis treatment? Cell Signal 26:1–8
17. Kong D, Zheng T, Zhang M, Wang D, Du S et al (2013) Static mechanical stress induces apoptosis in rat endplate chondrocytes through MAPK and mitochondria-dependent caspase activation signaling pathways. PLoS ONE 8:e69403
18. Abella V, Santoro A, Scotece M, Conde J, Lopez-Lopez V et al (2015) Non-dioxin-like polychlorinated biphenyls (PCB 101,

PCB 153 and PCB 180) induce chondrocyte cell death through multiple pathways. Toxicol Lett 234:13–19
19. Rasheed Z, Akhtar N, Haqqi TM (2010) Pomegranate extract inhibits the interleukin-1beta-induced activation of MKK-3, p38alpha-MAPK and transcription factor RUNX-2 in human osteoarthritis chondrocytes. Arthritis Res Ther 12:R195
20. Kong W, Wei J, Abidi P, Lin M, Inaba S et al (2004) Berberine is a novel cholesterol-lowering drug working through a unique mechanism distinct from statins. Nat Med 10:1344–1351
21. Qiu G, Song YH, Zeng P, Duan L, Xiao S (2013) Characterization of bacterial communities in hybrid upflow anaerobic sludge blanket (UASB)-membrane bioreactor (MBR) process for berberine antibiotic wastewater treatment. Bioresour Technol 142:52–62
22. Mo C, Wang L, Zhang J, Numazawa S, Tang H et al (2014) The crosstalk between Nrf2 and AMPK signal pathways is important for the anti-inflammatory effect of berberine in LPS-stimulated macrophages and endotoxin-shocked mice. Antioxid Redox Signal 20:574–588
23. Tsang CM, Cheung YC, Lui VW, Yip YL, Zhang G et al (2013) Berberine suppresses tumorigenicity and growth of nasopharyngeal carcinoma cells by inhibiting STAT3 activation induced by tumor associated fibroblasts. BMC Cancer 13:619
24. Zhang YJ, Yang SH, Li MH, Iqbal J, Bourantas CV et al (2014) Berberine attenuates adverse left ventricular remodeling and cardiac dysfunction after acute myocardial infarction in rats: role of autophagy. Clin Exp Pharmacol Physiol 41:995–1002
25. Domitrovic R, Cvijanovic O, Pernjak-Pugel E, Skoda M, Mikelic L et al (2013) Berberine exerts nephroprotective effect against cisplatin-induced kidney damage through inhibition of oxidative/nitrosative stress, inflammation, autophagy and apoptosis. Food Chem Toxicol 62:397–406
26. Moon PD, Jeong HS, Chun CS, Kim HM (2011) Baekjeolyusin-tang and its active component berberine block the release of collagen and proteoglycan from IL-1beta-stimulated rabbit cartilage and down-regulate matrix metalloproteinases in rabbit chondrocytes. Phytother Res 25:844–850
27. Hu PF, Chen WP, Tang JL, Bao JP, Wu LD (2011) Protective effects of berberine in an experimental rat osteoarthritis model. Phytother Res 25:878–885
28. Zhao H, Zhang T, Xia C, Shi L, Wang S et al (2014) Berberine ameliorates cartilage degeneration in interleukin-1beta-stimulated rat chondrocytes and in a rat model of osteoarthritis via Akt signalling. J Cell Mol Med 18:283–292
29. Hayami T, Pickarski M, Zhuo Y, Wesolowski GA, Rodan GA et al (2006) Characterization of articular cartilage and subchondral bone changes in the rat anterior cruciate ligament transection and meniscectomized models of osteoarthritis. Bone 38:234–243
30. Wang CJ, Huang CY, Hsu SL, Chen JH, Cheng JH (2014) Extracorporeal shockwave therapy in osteoporotic osteoarthritis of the knee in rats: an experiment in animals. Arthritis Res Ther 16:R139
31. Rautiainen J, Nissi MJ, Liimatainen T, Herzog W, Korhonen RK et al (2014) Adiabatic rotating frame relaxation of MRI reveals early cartilage degeneration in a rabbit model of anterior cruciate ligament transection. Osteoarthr Cartil 22:1444–1452
32. Simoes Pires EN, Frozza RL, Hoppe JB, Menezes Bde M, Salbego CG (2014) Berberine was neuroprotective against an in vitro model of brain ischemia: survival and apoptosis pathways involved. Brain Res 1557:26–33
33. Li MH, Zhang YJ, Yu YH, Yang SH, Iqbal J et al (2014) Berberine improves pressure overload-induced cardiac hypertrophy and dysfunction through enhanced autophagy. Eur J Pharmacol 728:67–76
34. Wang F, Wu L, Li L, Chen S (2014) Monotropein exerts protective effects against IL-1beta-induced apoptosis and catabolic responses on osteoarthritis chondrocytes. Int Immunopharmacol 23:575–580
35. Maia-de-Oliveira JP, Lobao-Soares B, Baker GB, Dursun SM, Hallak JE (2014) Sodium nitroprusside, a nitric oxide donor for novel treatment of schizophrenia, may also modulate dopaminergic systems. Schizophr Res 159:558–559
36. Guo S, Ashina M, Olesen J, Birk S (2013) The effect of sodium nitroprusside on cerebral hemodynamics and headache in healthy subjects. Cephalalgia 33:301–307
37. Hu Z, Jiao Q, Ding J, Liu F, Liu R et al (2011) Berberine induces dendritic cell apoptosis and has therapeutic potential for rheumatoid arthritis. Arthritis Rheum 63:949–959
38. Pandareesh MD, Anand T (2014) Neuroprotective and anti-apoptotic propensity of Bacopa monniera extract against sodium nitroprusside induced activation of iNOS, heat shock proteins and apoptotic markers in PC12 cells. Neurochem Res 39:800–814
39. de Andres MC, Maneiro E, Martin MA, Arenas J, Blanco FJ (2013) Nitric oxide compounds have different effects profiles on human articular chondrocyte metabolism. Arthritis Res Ther 15:R115
40. Haudenschild DR, Chen J, Pang N, Steklov N, Grogan SP et al (2011) Vimentin contributes to changes in chondrocyte stiffness in osteoarthritis. J Orthop Res 29:20–25
41. Gomez R, Conde J, Scotece M, Lopez V, Lago F et al (2014) Endogenous cannabinoid anandamide impairs cell growth and induces apoptosis in chondrocytes. J Orthop Res 32:1137–1146
42. Husa M, Petursson F, Lotz M, Terkeltaub R, Liu-Bryan R (2013) C/EBP homologous protein drives pro-catabolic responses in chondrocytes. Arthritis Res Ther 15:R218
43. Wang Y, Huang Y, Lam KS, Li Y, Wong WT et al (2009) Berberine prevents hyperglycemia-induced endothelial injury and enhances vasodilatation via adenosine monophosphate-activated protein kinase and endothelial nitric oxide synthase. Cardiovasc Res 82:484–492
44. Chen K, Li G, Geng F, Zhang Z, Li J et al (2014) Berberine reduces ischemia/reperfusion-induced myocardial apoptosis via activating AMPK and PI3 K-Akt signaling in diabetic rats. Apoptosis 19:946–957
45. Yan F, Wang L, Shi Y, Cao H, Liu L et al (2012) Berberine promotes recovery of colitis and inhibits inflammatory responses in colonic macrophages and epithelial cells in DSS-treated mice. Am J Physiol Gastrointest Liver Physiol 302:G504–G514